Journal of Molecular Liquids 245 (2017) 35–41

Contents lists available at ScienceDirect

Journal of Molecular Liquids

journal homepage: www.elsevier.com/locate/molliq

Statistical geometry characterization of global structure of TMAO and TBA aqueous solutions

A.V. Anikeenko, E.D. Kadtsyn, N.N. Medvedev *

Institute of Chemical Kinetics and Combustion, SB RAS, 630090 Novosibirsk, Russia
Novosibirsk State University, Novosibirsk, Russia

ARTICLE INFO

Article history:
Received 17 February 2017
Received in revised form 30 May 2017
Accepted 1 June 2017
Available online 1 June 2017

Keywords:
Structure of solutions
Voronoi method
Cluster analysis
Molecular dynamics simulation
TMAO aqueous solutions

ABSTRACT

We study the spatial distribution of trimethylamine-*N*-oxide (TMAO) and *tert*-butyl alcohol (TBA) molecules in aqueous solutions at low concentrations using molecular dynamics simulation, Voronoi-Delaunay method, and statistical cluster analysis. A comparison of these solutions with the systems of randomly distributed hard spheres is carried out. It is shown that TMAO molecules are generally distributed like random spheres. On the contrary, the distribution of TBA substantially differs from the random one, being the result of the self-association process in TBA solutions. Thus, using the methods of statistical geometry and systems of random spheres as a reference system, one can carry out a quantitative characterization of a global structure of a solution to describe general features of the spatial distribution of the solute molecules.

1. Introduction

Aqueous solutions of trimethylamine-*N*-oxide (TMAO) and *tert*-butyl alcohol (TBA) are the objects of many investigations by both experimental [1–13] and computer simulation methods [14–19]. TBA is an example of a simple amphiphilic molecule. Its solutions show nontrivial structural changes with concentration. It is believed that at low concentrations a TBA molecule "stabilizes" the surrounding water, i.e., owing to the presence of compact hydrophobic part (three methyl groups), it forms a specific hydration shell [1,8]. With the increase of concentration, self-association of TBA molecules begins due to the hydrophobic interaction. This mechanism is confirmed by the observation of extremes and kinks at mole fraction of TBA 0.02–0.05 on the experimental curves of some thermodynamics and spectroscopic parameters obtained by different methods, see for example [1,5,6,12]. The next structural changes in TBA solutions occur at a mole fraction of 0.15–0.20. They are related to the onset of "micro-heterogeneity", i.e., the arising of areas with different ratio of TBA and water molecules [2,3,5,16,19].

Interest in TMAO comes from molecular biology. It is well-known as protective osmolyte. TMAO stabilizes the native structure of proteins, preventing it from the denaturing action of temperature, pressure or denaturants like urea [20–24]. Despite many studies, the mechanism of TMAO action on protein at the molecular level is still unclear [24–26].

Molecules of TMAO and TBA look similar. They have small hydrophilic parts while the hydrophobic ones are formed by three methyl groups. One can expect the same structure and properties of their solutions. However, unlike TBA, TMAO solutions do not have specific features depending on concentration. This was shown experimentally [12] and confirmed by computer simulation [14,15]. Obviously, properties of solutions depend not only on the structure of hydrophobic part of a solute molecule. TMAO molecule differs from TBA by the presence of a larger charge on the oxygen atom, by three strong hydrogen bonds with water [13], and also by a large dipole moment. The interaction of TMAO and TBA molecules with water is discussed in many works and studied by quantum chemistry methods [27,28].

In this paper, we leave aside the question of these interactions and do not discuss the origin of different structures of TMAO and TBA solutions. The purpose of the present work is a detailed analysis of the spatial structure of these solutions by means of molecular dynamics simulations.

Investigations of the solution structure are often limited to the study of hydration shells. This is because they directly reflect the solute-solvent interaction, which can be measured experimentally by different methods. At the next level of the structure description, solute clusters are considered. They can arise at rather low concentration due to specific interactions and grow at higher concentration. However, there is another aspect of the solution structure, namely, the spatial distribution of the solute molecules. We call it *global structure*. It reflects general features and motifs of the solution component distribution in space. Computer simulations open a way to study different aspects of the global structure [16,17,29–31].

* Corresponding author.
E-mail address: nikmed@kinetics.nsc.ru (N.N. Medvedev).

http://dx.doi.org/10.1016/j.molliq.2017.06.001
0167-7322/

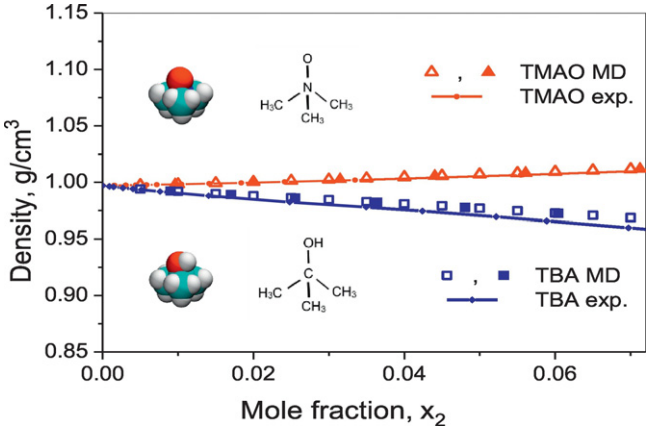

Fig. 1. The densities of aqueous solutions of TMAO and TBA at T = 300 K and P = 1 bar vs. concentration. Solid lines refer to experimental data [10,12]. Large symbols show the simulation values (empty symbols for the series A, filled – series B, see text). In the insert: molecular structure and van der Waals representation of the TMAO and TBA.

Note that solutions belong to the area of random spatial systems which are studied in different fields of sciences. Similar structural problems arise in physics of liquids, glasses, granular packing, in porous systems, see, e.g., books [32,33]. There are different approaches to such problems. One of them is based on the Voronoi-Delaunay tessellation, which is a universal geometrical tool for the description of mutual spatial arrangement of objects [34,35]. Another approach is the cluster analysis which selects clusters (groups) in a system of particles randomly distributed in space [32,33].

In the present paper, we use these approaches for the quantitative characterization of the spatial distribution of TMAO and TBA molecules in molecular dynamics models of their aqueous solutions at different concentrations. In order to estimate the degree of inhomogeneity of the solution, we carry out the comparison with systems of randomly distributed hard spheres with different density.

2. Models

2.1. Solutions

We have considered two series of simulations of aqueous solutions of TBA and TMAO for different concentrations. In the first one (A), each simulation box contains 100 solute molecules (TMAO or TBA) and the concentration ranges from 0.27 to 4.3 M, (mol/L). The simulation box for the lowest concentration has an edge length of 8.5 nm and contains 19,900 water molecules. The more concentrated solutions were made by removing the required number of water molecules and decreasing the box size. Thus, for example, the most concentrated solution of TMAO has a box edge length of 3.4 nm and contains 900 water molecules.

In the second series (B), each model contains 160 solute molecules and the concentration ranges from about 0.48 to 3.3 M. The box size varies from 8.2 to 4.3 nm, while the number of water molecules changes from 17,613 to 2085. The molecular dynamics calculations and the analysis were done using the same parameters, as specified below. As we found, there is no noticeable difference between simulation results from different series. The comparison of the calculated and experimental densities of the solutions is shown in Fig. 1. One can see quite a good agreement for all concentrations.

All simulations were performed using the GROMACS package, version 5.0.7 [36], on the 4th Generation Intel Core i7 processor with NVIDIA CUDA GPU acceleration. All-atom force field parameters for TMAO are taken from [37], and for OPLS-AA model of TBA from [38]. For water, the TIP4P/2005 model was used [39]. The Particle Mesh Ewald scheme with spacing of 0.12 nm was utilized for electrostatic interactions, and 1.0 nm short-range interactions cut-offs were used. Simulations were performed in the NPT ensemble using the v-rescale thermostat and the Parrinello-Rahman barostat [40,41] with relaxation times of 1 ps and 2 ps, respectively. Temperature and pressure were kept at 300 K and 1 bar. All bond lengths were constrained using the LINCS algorithm and the integration time step was set to 2 fs. Each simulation involved a 0.1 ns equilibration followed by a 100 ns production run. Configurations were saved to file each 10 ps.

Since the volume of the system in the NTP ensemble fluctuates, we use the mean values of the molar concentrations everywhere. The relative error of the mean molarity did not exceed 0.03% for all simulations when estimated by the block-averaging method.

2.2. Random spheres

The models of random spheres of different density were created by random sequential addition of hard spheres into empty simulation box with periodic boundary conditions. The diameter of spheres D was chosen to be 0.53 nm and the packing fraction was determined by the size of the box and by the given number of spheres. (Recall that packing fraction is the ratio of volume occupied by spheres to the volume of the system: $\eta = V_{sph} / V_{box}$). We have obtained also two series of simulations containing 160 and 1280 spheres for all densities η. One can think that models with hundred of spheres do not allow us to obtain good sampling. However, all statistical characteristics, in particular the volumes of Voronoi regions and their variance are practically identical in both series for all η. The number of independent configurations used for averaging was 10^5.

We have chosen the value for D as an optimal size for both the TMAO and the TBA molecules. This value corresponds approximately to the mid-point on the left slope of the first peaks of the $g(r)$ both for TMAO and for TBA, see Fig. 6 in Results section. Thereby, the value of $D =$ 0.53 nm is a good estimate of the "hard core" diameter for both the TMAO and the TBA. By representing our molecules as spheres of a given diameter, we are able to calculate the packing fraction η for the solutions. Thus, we can measure the concentration of the solutions either in mol/L, or as a mole fraction $x_2 = N_2/(N_2 + N_1)$ as well as with packing fraction η, i.e., as fraction of volume occupied by solute molecules represented as spheres of a given radius. These values for some of our systems are shown in Table 1.

System of random spheres with packing fractions ranging from 0 to 0.2 were simulated, in order to cover the whole range of concentration of the solutions investigated. The system with $\eta = 0$ was calculated using zero sphere diameter $D = 0$. In this case, the system corresponds to a random distribution of points, which is broadly studied in

Table 1
Correspondence between molar concentration c, packing fraction η, and molar fraction x_2 for TMAO and TBA solutions (only some models are presented).

Molar concentration, mol/L TBA, TMAO	0.27	0.53	1.27	2.35	3.22	4.05	4.30
Packing fraction η TBA, TMAO. $D = 0.53$ nm	0.013	0.025	0.06	0.11	0.15	0.19	0.20
Mole fraction x_2 TBA	0.005	0.01	0.025	0.050	0.075	0.10	0.11
TMAO	0.005	0.01	0.025	0.048	0.070	0.095	0.10

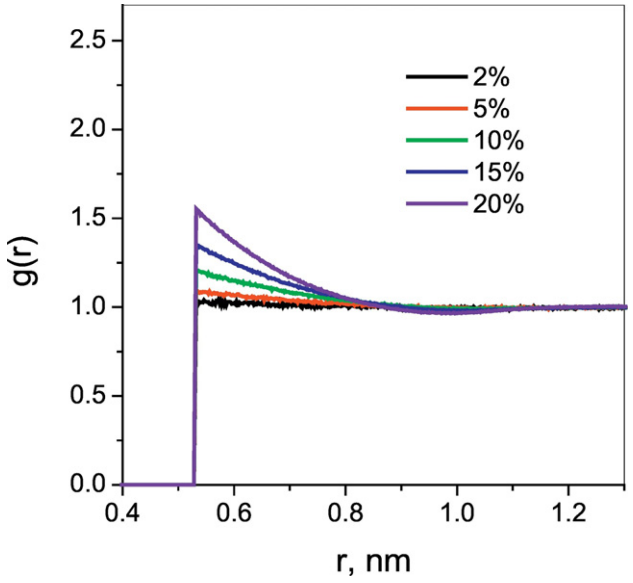

Fig. 2. Pair correlation functions for system of random spheres with diameter $D = 0.53$ nm for packing fractions $\eta = 0.02$, 0.05, 0.1, 0.15 and 0.2.

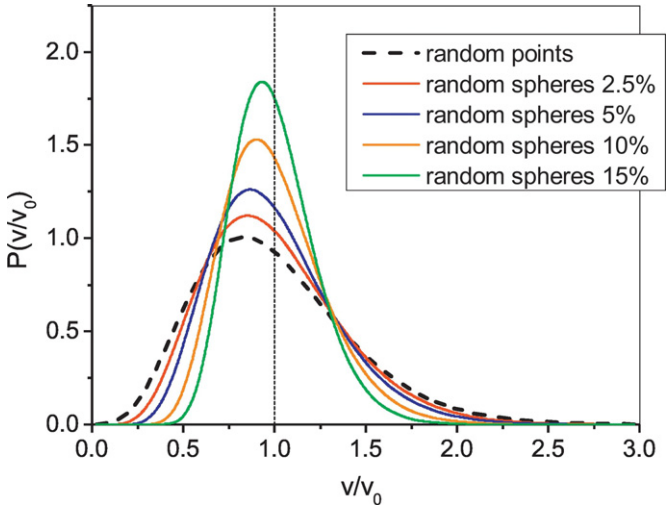

Fig. 4. Distributions of Voronoi region volumes for systems of random spheres with different packing fractions. All distributions are normalized to the mean volume (vertical line at 1). Dashed curve corresponds to the distribution of random points ($\eta = 0$).

mathematics [42]. In Fig. 2 the pair correlation functions for systems of random spheres at different packing fractions are shown.

At these densities, our systems can be considered as "a gas" or "a fluid" of hard spheres. Recall that for random points with uniform spatial distribution the pair correlation function $g(r)$ is equal to 1 for all r. For hard spheres at low packing fractions, $g(r)$ is also almost equal to 1 for all $r > D$. However, if the packing fraction is a few percent, one can discern the appearance of the first peak which is growing monotonically with packing fraction, see Fig. 2. However, packing effects leading to oscillations of $g(r)$ do not appear yet. For the highest density $\eta = 0.2$, only a very weak minimum can be recognized after the first maximum. One can only see a small hint to the appearance of a minimum after the first maximum.

3. Methods

3.1. Voronoi regions

To investigate the mutual spatial arrangement of particles, one can use the Voronoi-Delaunay tessellation [34,35]. In the present work, we calculate volumes of Voronoi regions. Recall that the Voronoi region defines the volume of space, which is closer to a given atom than to any other atoms of the system. Fig. 3 illustrates 2D Voronoi regions for different systems. One can see that they are sensitive to the spatial distribution of particles.

The distributions of Voronoi volumes for random spheres are shown in Fig. 4. In order to compare distributions for models with different packing fraction we normalized our distributions to the mean Voronoi volume for each system. Thereby the mean value for each distribution is equal to 1 in Fig. 4 (marked by vertical line). One can see that the denser the system the narrower and more symmetrical the distribution; as it can also be observed in Fig. 3. To compare random sphere systems with our solutions we use the dispersion of the normalized distributions of Voronoi volumes: $Var[v/v_0]\langle(v/v_0 - 1)^2\rangle$, where v_0 is the mean volume of Voronoi regions in the system. When the density increases, the dispersion decreases strongly (about six times in our range of densities, see below).

When working with the solutions, we calculated the Voronoi regions for the centers of solute molecules. The nitrogen atom and the tertiary carbon atom were chosen as molecular centers for TMAO and TBA, respectively. Water molecules were ignored in these calculations, i.e., we carried out the decomposition of solution volume using the solute molecules only. The Python libraries *mdtraj* [43] and *tess* [44,45] were employed for the calculation of Voronoi tessellation from the molecular dynamics trajectories.

3.2. Clusters

The problem of cluster detection and analysis in systems of particles is well known in physics and related sciences [32,33]. In our study, we use a simple method to define clusters: the cluster is formed by those

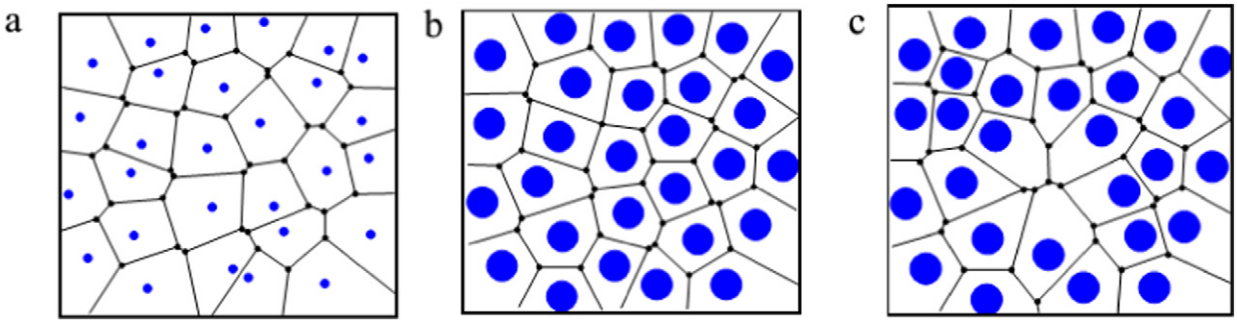

Fig. 3. Two-dimensional illustration of Voronoi tessellation for systems of random points and spheres with finite radius. a) system of points, b) homogeneous random spheres, c) inhomogeneously distributed spheres.

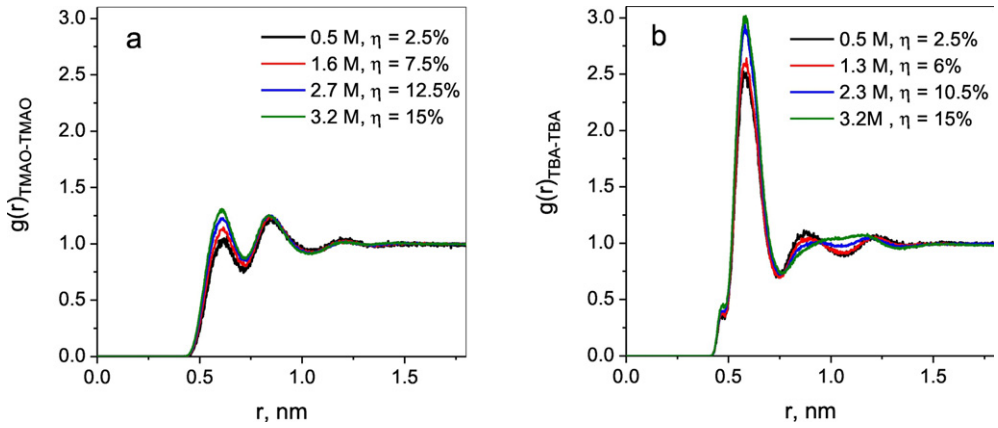

Fig. 5. Molecule-molecule pair correlation functions for TMAO (a) and TBA (b) aqueous solutions at different concentrations. Central N and C atoms are used as the centers of TMAO and TBA molecules.

particles which are spaced apart closer than the given cutoff distance, i.e., if the particle is close to at least one particle of the cluster, it also belongs to this cluster. Determination of clusters was performed using the program *clustsize* from the GROMACS 5.0.7 package [36]. All clusters and their size (number of particles in the cluster) were identified for each model configuration. The mean cluster size for a given model was calculated by averaging over many configurations of the model: 10^5 independent configurations for random spheres for each packing fraction, and 10^4 frames of a molecular dynamics trajectory for each solution. Note that the calculation of the mean cluster size also takes into account clusters of size 1, i.e., isolated particles, which do not have close neighbors.

4. Results

Primary information about the spatial organization of the system of particles can be obtained via the pair correlation functions. Pair correlation functions calculated for the centers of the molecules in solution are shown in Fig. 5.

Firstly, let us note that the first peak for TMAO is very low. It is lower than the second maximum of the TMAO and substantially lower than the first maximum for TBA. In both cases, the heights of the first peaks increase with increasing concentration, but the subsequent oscillations behave differently. In TMAO they practically do not change, and in the TBA solution, the second and third peaks begin to merge into one, see 3.2 M curve in Fig. 5b. A small prepeak at values of around 0.45 nm on TBA-TBA $g(r)$ curves (Figs. 5b and 6) corresponds to the hydrogen bonded TBA molecules.

In order to understand the change of $g(r)$ with concentration as well as differences between TMAO and TBA, let us compare $g(r)$ of TMAO and TBA with random spheres, Fig. 6.

The presence of the second and third peaks in $g(r)$ for solutions is caused by the structuring effect of the solvent. The structure of water defines some preferential distances between solute molecules. The first peak is obviously determined by direct van der Waals contact of the molecules. In this case, each molecule is located in the hydration shell of another molecule. The second peak can be attributed to the "overlap" of hydration shells, i.e., to the case when only a "monolayer" of hydrated water molecules remains between the solute molecules. The third maximum, one might think, corresponds to the distance when the molecules "touch" with their hydration shells. Note that these preferential distances have nothing to do with the laws of packing of solute molecules alone. Indeed, the second and third maxima in solutions exist already at very low concentrations, at which the system of random spheres does not even exhibit the first peak, Fig. 6a.

The fraction of random spheres in contact increases with increasing density, as seen in Fig. 2. The same effect can be observed, for the TMAO and TBA solutions, in Fig. 5. Thus, the increase in the height of the first peak of $g(r)$ has a geometric cause. It largely determines the behavior of the first peak for TMAO. However, specific intermolecular interactions also govern the structure of the solutions. In particular, TBA molecules can form hydrogen bonds with each other. Moreover, the so-called hydrophobic interaction appears between them in water. This leads to the fact that the proportion of close molecules is greater than for a random distribution in space, and it explains why the first peak of $g(r)$ is so high in TBA solution even at low concentrations.

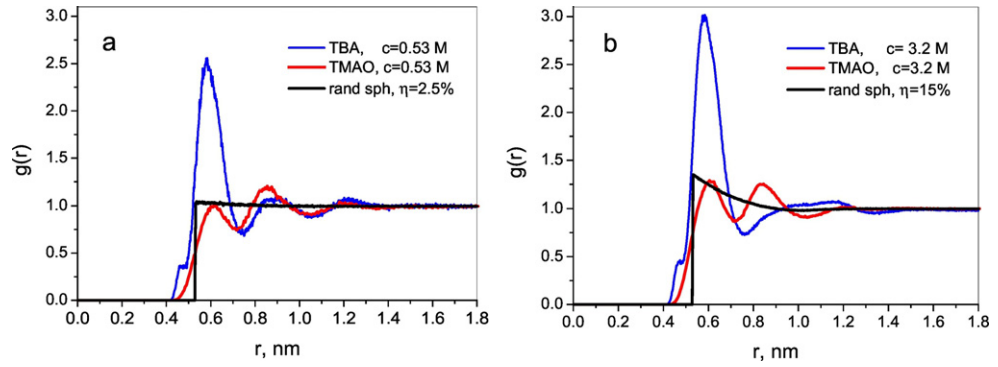

Fig. 6. Comparison of the pair correlation functions of TMAO (red), TBA (blue) and random hard spheres (black) at different concentrations. $\eta = 0.025$ ($c_{TMAO} = c_{TBA} = 0.53$ M, $x_{TMAO} = 1\%$, $x_{TBA} = 1\%$) (a), $\eta = 0.15$ ($c_{TMAO} = c_{TBA} = 3.2$ M, $x_{TMAO} = 7\%$, $x_{TBA} = 7.5\%$) (b).

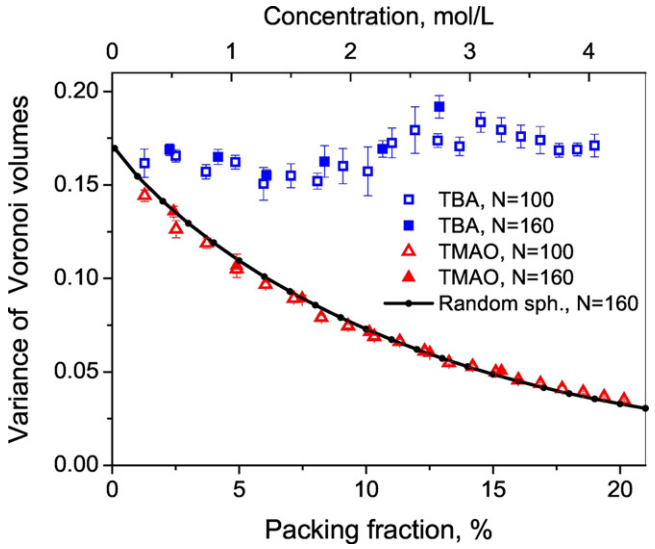

Fig. 7. Variance of normed Voronoi cell volume distributions for TBA (blue squares) and TMAO (red triangles) solute molecules in solution compared with random spheres (black line). Filled symbols correspond to models of solutions with 160 solute molecules, open symbols – 100 molecules, see text. Errors are estimated by block averaging method over the MD trajectory.

Using only the information from the $g(r)$ it is difficult to judge the distribution of molecules in space as a whole. The direct information about it can be obtained from the analysis of the Voronoi-Delaunay tessellation. Fig. 7 shows the variance of the Voronoi volumes depending on the concentration. To compare the solutions with the system of random spheres we estimated the degree of space filling for dissolved molecules, see Table 1. One can see that the curve for TMAO solutions agrees very well with the curve for the random spheres. This means that the TMAO molecules are arranged randomly in the solution over the range of the investigated concentrations. The presence of small oscillations on the $g(r)$ function in the solution (which are not present in random spheres), as we see, does not affect the general character of the distribution of molecules in space.

In the TBA solutions, the variance of Voronoi volumes behaves quite differently, at first it slightly decreases but then begins to grow. This behavior is understandable since the growth of the dispersion indicates the emergence of inhomogeneities, which arise from the association of TBA with increasing concentration.

What is surprising is that TMAO behaves like a system of random spheres, in spite of all intermolecular interactions, which can happen between real molecules. Fig. 8 shows the distribution of Voronoi region volumes.

It is clear that for both low and high concentrations there is a very good agreement between the distributions for TMAO and random spheres, as opposed to the TBA case, where there is a significant difference in the distribution.

Fig. 9 shows the results of our cluster analysis of the solutions and of the system of random spheres. For cluster selection, we use the distance criterion.

First, we considered two particles as being connected if the distance between their centers was less than 0.58 nm (it is an approximated position of the first peaks at $g(r)$ for both TMAO and TBA solutions). As the second criterion, we took a distance of 0.72 nm, (first minimum of $g(r)$). In this case, any particle in the nearest shell of the molecule is meant to be included into the cluster.

Regardless of the criterion used, we get a very interesting result: the mean size of the clusters in TMAO solutions is almost the same as in the system of random spheres for all densities. On the contrary, the size of clusters in TBA solution is much larger. Thereby, this statistical analysis also shows that TMAO molecules are distributed in solution like random spheres at the same packing fraction. By this property, TMAO solutions strongly differ from TBA, where due to specific intermolecular interactions, the spatial distribution of molecules is different.

5. Conclusions

We investigated the general character of the spatial distribution of TMAO molecules in aqueous solution at rather low (biologically relevant) concentrations and compared it with TBA solutions and with random spheres. For this purpose, we used the molecular dynamics models of the solutions at different concentrations and the systems of random spheres with the corresponding densities.

It was shown that TMAO molecules are distributed in the solution like random spheres. This result follows from the coincidence of Voronoi volumes of the molecules in solutions and in the systems of random spheres, as well as from the coincidence of the mean size of the clusters. However, for TBA solutions, the calculated characteristics differ substantially from random spheres. This phenomenon is related to the known property of TBA to form associates in the solution. The first peak of the

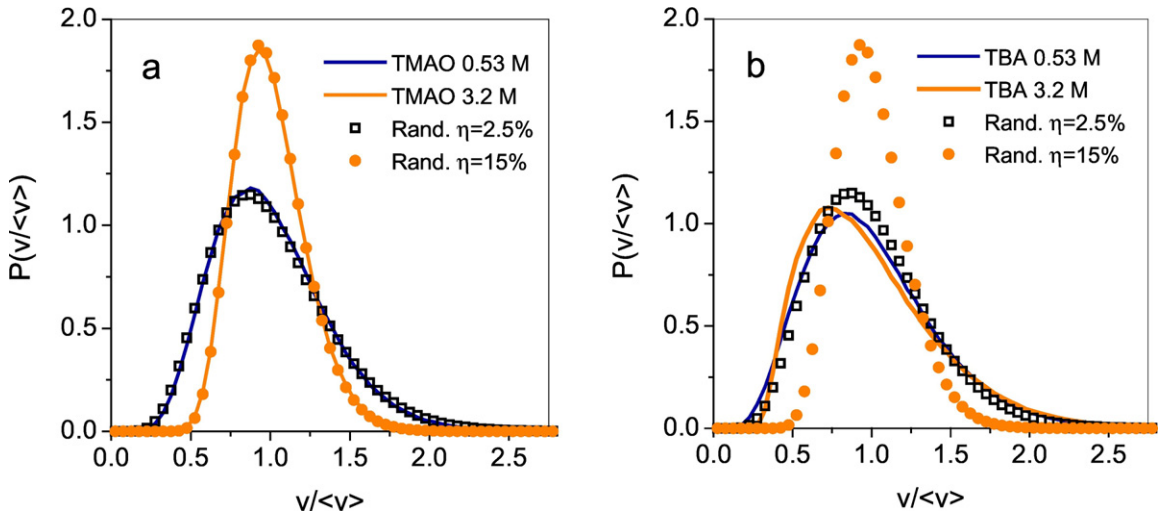

Fig. 8. Voronoi volume distribution for TMAO (a) and TBA (b) in solutions of different concentrations (solid lines) in comparison with random spheres (symbols) at the corresponding densities.

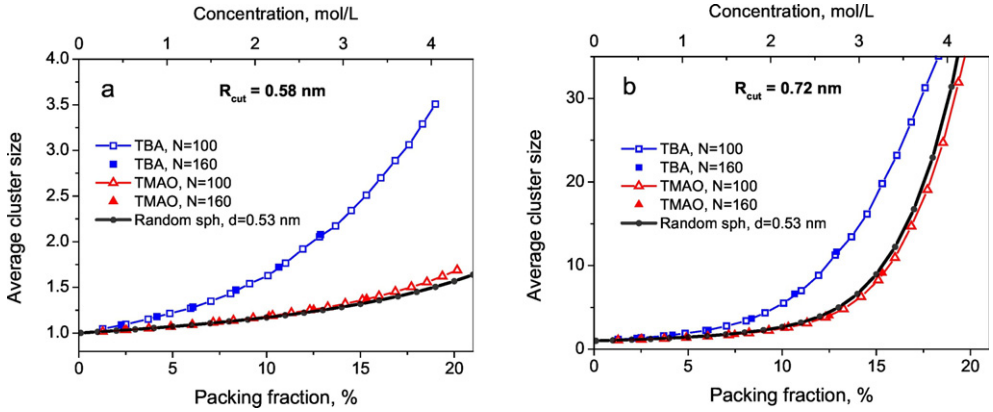

Fig. 9. The mean size of the clusters in TMAO (red) and TBA (blue) solutions, and in the system of random spheres (black line) vs. density of the system. Cutoff distances for including particles into cluster were 0.58 nm (a) and 0.72 nm (b).

center-center pair correlation function $g(r)$ for TMAO is weak and even lower than the second one at low concentrations. The growth of this peak with concentration repeats the trivial behavior of the first peak in the system of random spheres. In the TBA solution, the first peak is much higher, resulting from the specific interactions between TBA molecules.

In solutions, the pair correlation function shows also a marked second and third peak. For the system of random spheres at the studied densities, these peaks are absent. Such preferred distances in solutions are caused by the structuring effect of water. However, the influence of water on the "local" order of the solute molecules does not affect the global structure of the solutions.

The sensitivity of the spatial distribution of random spheres to the change of density, even at low packing fractions, shows that one should compare structural properties of the solution with the system of random spheres (bodies) rather than with the system of random points.

Acknowledgements

Financial support from grant RFFI (No. 15-03-03329) is gratefully acknowledged.

References

[1] F. Franks, D.J.G. Ives, The structural properties of alcohol–water mixtures, Q. Rev. Chem. Soc. 20 (1966) 1–44, http://dx.doi.org/10.1039/QR9662000001.
[2] K. Iwasaki, T. Fujiyama, Light-scattering study of clathrate hydrate formation in binary mixtures of tert-butyl alcohol and water, J. Phys. Chem. 81 (1977) 1908–1912, http://dx.doi.org/10.1021/j100535a005.
[3] K. Nishikawa, H. Hayashi, T. Iijima, Temperature dependence of the concentration fluctuation, the Kirkwood-Buff parameters, and the correlation length of tert-butyl alcohol and water mixtures studied by small-angle x-ray scattering, J. Phys. Chem. 93 (1989) 6559–6565, http://dx.doi.org/10.1021/j100354a054.
[4] P.K. Kipkemboi, A.J. Easteal, Densities and viscosities of binary aqueous mixtures of nonelectrolytes: tert-butyl alcohol and tert-butylamine, Can. J. Chem. 72 (1994) 1937–1945, http://dx.doi.org/10.1139/v94-247.
[5] D. Glew, H. Mak, N. Rath, Aqueous non-electrolyte solutions: part VII. Water shell stabilization by interstitial nonelectrolytes, in: A.K. Covington, P. Jones (Eds.), Hydrogen-bonded Solvent Systems, Taylor & Francis, London 1968, pp. 195–210.
[6] M. Freda, G. Onori, A. Santucci, Infrared study of the hydrophobic hydration and hydrophobic interactions in aqueous solutions of tert-butyl alcohol and trimethylamine-n-oxide, J. Phys. Chem. B 105 (2001) 12714–12718, http://dx.doi.org/10.1021/jp011673m.
[7] A. Di Michele, M. Freda, G. Onori, A. Santucci, Hydrogen bonding of water in aqueous solutions of trimethylamine-N-oxide and tert-butyl alcohol: a near-infrared spectroscopy study, J. Phys. Chem. A 108 (2004) 6145–6150, http://dx.doi.org/10.1021/jp0494990.
[8] R. Sinibaldi, C. Casieri, S. Melchionna, G. Onori, A.L. Segre, S. Viel, L. Mannina, F. De Luca, The role of water coordination in binary mixtures. A study of two model amphiphilic molecules in aqueous solutions by molecular dynamics and NMR, J. Phys. Chem. B 110 (2006) 8885–8892, http://dx.doi.org/10.1021/jp056897.
[9] C.A. Yinnon, T.A. Yinnon, Domains in aqueous solutions: theory and experimental evidence, Mod. Phys. Lett. B 23 (2009) 1959–1973, http://dx.doi.org/10.1142/S0217984909020138.
[10] G.I. Egorov, D.M. Makarov, Densities and volume properties of (water + tert-butanol) over the temperature range of (274.15 to 348.15) K at pressure of 0.1 MPa, J. Chem. Thermodyn. 43 (2011) 430–441, http://dx.doi.org/10.1016/j.jct.2010.10.018.
[11] J. Rösgen, R. Jackson-Atogi, Volume exclusion and H-bonding dominate the thermodynamics and solvation of trimethylamine-N-oxide in aqueous urea, J. Am. Chem. Soc. 134 (2012) 3590–3597, http://dx.doi.org/10.1021/ja211530n.
[12] D.M. Makarov, G.I. Egorov, A.M. Kolker, Density and volumetric properties of aqueous solutions of trimethylamine N-oxide in the temperature range from (278.15 to 323.15) K and at pressures up to 100 MPa, J. Chem. Eng. Data 60 (2015) 1291–1299, http://dx.doi.org/10.1021/je500977g.
[13] Y. Sasaki, Y. Horikawa, T. Tokushima, K. Okada, M. Oura, M. Aida, Hydration structure of trimethylamine N-oxide in aqueous solutions revealed by soft X-ray emission spectroscopy and chemometric analysis, Phys. Chem. Chem. Phys. 18 (2016) 27648–27653, http://dx.doi.org/10.1039/C6CP03750J.
[14] A. Fornili, M. Civera, M. Sironi, S.L. Fornili, Molecular dynamics simulation of aqueous solutions of trimethylamine-N-oxide and tert-butyl alcohol, Phys. Chem. Chem. Phys. 5 (2003) 4905–4910, http://dx.doi.org/10.1039/b308248b.
[15] S. Paul, G.N. Patey, Why tert-butyl alcohol associates in aqueous solution but trimethylamine-N-oxide does not, J. Phys. Chem. B 110 (2006) 10514–10518, http://dx.doi.org/10.1021/jp0609378.
[16] A. Perera, R. Mazighi, B. Kežić, Fluctuations and micro-heterogeneity in aqueous mixtures, J. Chem. Phys. 136 (2012) 174516, http://dx.doi.org/10.1063/1.4707745.
[17] R. Gupta, G.N. Patey, Aggregation in dilute aqueous tert-butyl alcohol solutions: insights from large-scale simulations, J. Chem. Phys. 137 (2012), 034509. http://dx.doi.org/10.1063/1.4731248.
[18] S. Banerjee, J. Furtado, B. Bagchi, Fluctuating micro-heterogeneity in water–tert-butyl alcohol mixtures and lambda-type divergence of the mean cluster size with phase transition-like multiple anomalies, J. Chem. Phys. 140 (2014) 194502, http://dx.doi.org/10.1063/1.4874637.
[19] D. Subramanian, C.T. Boughter, J.B. Klauda, B. Hammouda, M.A. Anisimov, Mesoscale inhomogeneities in aqueous solutions of small amphiphilic molecules, Faraday Discuss. 167 (2013) 217–238, http://dx.doi.org/10.1039/c3fd00070b.
[20] T.-Y. Lin, S.N. Timasheff, Why do some organisms use a urea-methylamine mixture as osmolyte? Thermodynamic compensation of urea and trimethylamine N-oxide interactions with protein, Biochemistry 33 (1994) 12695–12701, http://dx.doi.org/10.1021/bi00208a021.
[21] D.W. Bolen, I.V. Baskakov, The osmophobic effect: natural selection of a thermodynamic force in protein folding, J. Mol. Biol. 310 (2001) 955–963, http://dx.doi.org/10.1006/jmbi.2001.4819.
[22] P.H. Yancey, M.D. Rhea, K.M. Kemp, D.M. Bailey, Trimethylamine oxide, betaine and other osmolytes in deep-sea animals: depth trends and effects on enzymes under hydrostatic pressure, Cell. Mol. Biol. (Noisy-le-Grand) 50 (2004) 371–37615529747.
[23] Q. Zou, B.J. Bennion, V. Daggett, K.P. Murphy, The molecular mechanism of stabilization of proteins by TMAO and its ability to counteract the effects of urea, J. Am. Chem. Soc. 124 (2002) 1192–1202, http://dx.doi.org/10.1021/ja004206b.
[24] D.R. Canchi, A.E. García, Cosolvent effects on protein stability, Annu. Rev. Phys. Chem. 64 (2013) 273–293, http://dx.doi.org/10.1146/annurev-physchem-040412-110156.
[25] J. Hunger, N. Ottosson, K. Mazur, M. Bonn, H.J. Bakker, Water-mediated interactions between trimethylamine-N-oxide and urea, Phys. Chem. Chem. Phys. 17 (2015) 298–306, http://dx.doi.org/10.1039/C4CP02709D.
[26] N. Smolin, V.P. Voloshin, A.V. Anikeenko, A. Geiger, R. Winter, N.N. Medvedev, TMAO and urea in the hydration shell of the protein SNase, Phys. Chem. Chem. Phys. 19 (2017) 6345–6357, http://dx.doi.org/10.1039/C6CP07903B.
[27] S. Imoto, H. Forbert, D. Marx, Water structure and solvation of osmolytes at high hydrostatic pressure: pure water and TMAO solutions at 10 kbar versus 1 bar, Phys. Chem. Chem. Phys. 17 (2015) 24224–24237, http://dx.doi.org/10.1039/C5CP03069B.
[28] K. Usui, J. Hunger, M. Sulpizi, T. Ohto, M. Bonn, Y. Nagata, Ab initio liquid water dynamics in aqueous TMAO solution, J. Phys. Chem. B 119 (2015) 10597–10606, http://dx.doi.org/10.1021/acs.jpcb.5b02579.
[29] H. Lee, J.-H. Choi, P.K. Verma, M. Cho, Spectral graph analyses of water hydrogen-bonding network and osmolyte aggregate structures in osmolyte–water solutions,

J. Phys. Chem. B 119 (2015) 14402–14412, http://dx.doi.org/10.1021/acs.jpcb.5b08029.
[30] M. Požar, J.-B. Seguier, J. Guerche, R. Mazighi, L. Zoranić, M. Mijaković, B. Kežić-Lovrinčević, F. Sokolić, A. Perera, Simple and complex disorder in binary mixtures with benzene as a common solvent, Phys. Chem. Chem. Phys. 17 (2015) 9885–9898, http://dx.doi.org/10.1039/C4CP05970K.
[31] M. Požar, B. Lovrinčević, L. Zoranić, T. Primorać, F. Sokolić, A. Perera, Micro-heterogeneity versus clustering in binary mixtures of ethanol with water or alkanes, Phys. Chem. Chem. Phys. 18 (2016) 23971–23979, http://dx.doi.org/10.1039/C6CP04676B.
[32] C.C. Aggarwal, C.K. Reddy (Eds.), Data Clustering: Algorithms and Applications, Taylor & Francis Group, New York, 2014.
[33] J. Illian, A. Penttinen, H. Stoyan, D. Stoyan, Statistical Analysis and Modelling of Spatial Point Patterns, John Wiley & Sons Ltd, Chichester, 2008.
[34] A. Okabe, B. Boots, K. Sugihara, S.N. Chiu, Spatial Tessellations: Concepts and Applications of Voronoi Diagrams, 2nd ed. J. Wiley & Sons, Chichester, 2000.
[35] N.N. Medvedev, The Voronoi-Delaunay Method in the Structural Investigation of Non-crystalline Systems, SB RAS, Novosibirsk, 2000 (in Russian).
[36] S. Páll, M.J. Abraham, C. Kutzner, B. Hess, E. Lindahl, Tackling exascale software challenges in molecular dynamics simulations with GROMACS, in: S. Markidis, E. Laure (Eds.), Solving Software Challenges for Exascale, Springer International Publishing, Cham 2015, pp. 3–27, http://dx.doi.org/10.1007/978-3-319-15976-8_1.
[37] C. Hölzl, P. Kibies, S. Imoto, R. Frach, S. Suladze, R. Winter, D. Marx, D. Horinek, S.M. Kast, Design principles for high–pressure force fields: aqueous TMAO solutions from ambient to kilobar pressures, J. Chem. Phys. 144 (2016) 144104, http://dx.doi.org/10.1063/1.4944991.
[38] C. Caleman, P.J. van Maaren, M. Hong, J.S. Hub, L.T. Costa, D. van der Spoel, Force field benchmark of organic liquids: density, enthalpy of vaporization, heat capacities, surface tension, isothermal compressibility, volumetric expansion coefficient, and dielectric constant, J. Chem. Theory Comput. 8 (2012) 61–74, http://dx.doi.org/10.1021/ct200731v.
[39] J.L.F. Abascal, C. Vega, A general purpose model for the condensed phases of water: TIP4P/2005, J. Chem. Phys. 123 (2005) 234505, http://dx.doi.org/10.1063/1.2121687.
[40] G. Bussi, D. Donadio, M. Parrinello, Canonical sampling through velocity rescaling, J. Chem. Phys. 126 (2007), 014101. http://dx.doi.org/10.1063/1.2408420.
[41] M. Parrinello, A. Rahman, Polymorphic transitions in single crystals: a new molecular dynamics method, J. Appl. Phys. 52 (1981) 7182, http://dx.doi.org/10.1063/1.328693.
[42] J. Møller, Lectures on Random Voronoi Tessellations, Springer-Verlag, New York, 1994.
[43] R.T. McGibbon, K.A. Beauchamp, M.P. Harrigan, C. Klein, J.M. Swails, C.X. Hernández, C.R. Schwantes, L.-P. Wang, T.J. Lane, V.S. Pande, MDTraj: a modern open library for the analysis of molecular dynamics trajectories, Biophys. J. 109 (2015) 1528–1532, http://dx.doi.org/10.1016/j.bpj.2015.08.015.
[44] Tess 0.2, https://pypi.python.org/pypi/tess/0.2 (accessed January 31, 2017).
[45] C.H. Rycroft, VORO++: a three-dimensional Voronoi cell library in C++, Chaos 19 (2009), 041111. http://dx.doi.org/10.1063/1.3215722.